Effect of LET Parameters Combination in Relative Permeability towards Core and Field Scale Simulation

Wilson Wiranda[1*], *Kurdistan* Chawsin[1], and *Rolf* Myhr[1]

[1]PRORES AS, 7041 Trondheim, Norway

Abstract. The LET correlation has been widely used to match the relative permeability obtained from laboratory experiments and for upscaling field-scale reservoir simulation. The reason is that the LET correlation provides a versatile formula to match the data points. This formula utilizes up to 3 parameters for each curve, i.e., L, E and T. However, due to this flexibility, different combinations of the L-E-T parameters could create near-identical relative permeability curves. In this study, we document a methodology for generating multiple LET combinations that match the laboratory data. Our investigations show that the L versus log(E) and L versus T follow a linear trend to generate "similar" relative permeability curves. To evaluate the impact of various LET combinations on core and field-scale simulations, two coreflood and field-scale sensitivity studies are conducted utilizing benchmark models of an oil-water system from UNISIM-I and a three-phase system from the Norne field. The coreflooding simulation is completed under steady-state conditions. In the case of UNISIM-I data, the coreflooding simulation shows only a recovery factor difference of 0.68% with different LET combinations. Using these combinations, the field-scale simulation shows a recovery range of 23.70% – 23.77%. For the Norne field, coreflooding simulations for both water-oil and gas-oil systems were considered. The coreflooding simulation result for the water-oil system shows a 3.94% recovery factor difference and the gas-oil system shows a 4.84% recovery factor difference. In this case, the field simulation yields a wider range of recovery factor compared to the UNISIM-I model, ranging from 42.52% to 43.69%. This effect was investigated thoroughly with the end-of-field simulation and the relative permeability difference. This study indicates that the effect of different LET combinations on the relative permeability curves and eventual recovery factor can initially be observed through coreflooding simulation. Moreover, lower L parameters are observed to increase the relative permeability at the endpoint, which may affect the development and decision-making processes for brownfields. Finally, this study presents a variety of LET combinations to fit laboratory data that could potentially serve as a method for quality-controlling the LET combinations used in the simulation.

1 Introduction

Relative permeability is one of the important variables in reservoir simulation, which enables the understanding of two-phase flow in the reservoir and is crucial in determining reservoir performance [1]. To obtain relative permeability data, coreflooding is frequently performed by injecting water or gas into an oil-saturated sample at initial water saturation condition.

The result of coreflooding is usually presented as differential pressure and production volume of the displaced fluid. Analytical relative permeability is obtained based on the coreflooding results. The number of saturation points where analytical relative permeability can be derived are dependent to the type of coreflooding experiment (**Fig. 1**).

The data obtained from coreflooding is used as input into coreflooding simulation to validate and obtain the parameterized relative permeability curve.

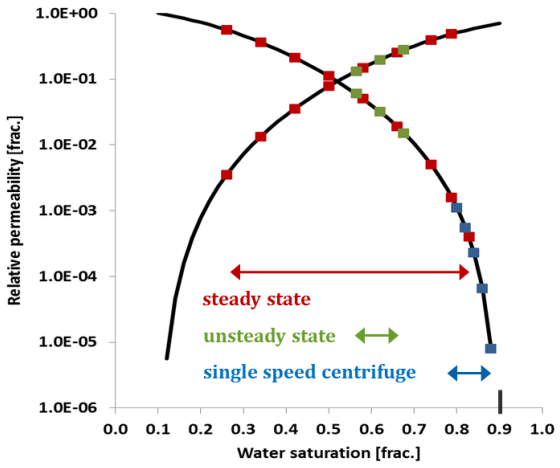

Fig. 1. Relative permeability experiments and the saturation range in which they provide information. [1]

There are several correlation methods that can be utilized for parametrization of experimental relative permeability data [2-6], from which Corey and LET methods are among the most

* Corresponding author: wilsonwiranda@outlook.com

popular ones. The Corey model is a simple power law function that uses a single empirical parameter to match the experimental data. However, capturing the entire saturation range using only one parameter can get challenging in field applications. The LET relative permeability correlation is widely used to match relative permeability data due to its versatility to match the data points. The LET formula utilizes three parameters for each curve, i.e. L, E and T.

With the flexibility that LET relative permeability correlation offers, it is possible to generate a different set of L, E and T combinations to obtain near-identical relative permeability curves that match with the coreflooding data.

This study demonstrates a method to generate the near-identical relative permeability curves with different L, E and T combinations and the impact on coreflooding simulation as well as field-scale simulation. In combination with field trend models, introduced by Ebeltoft et. al. [1], this method can be used to adjust the relative permeability parameters for a better understanding of the possible parameter combinations, and finally reducing the field level dynamic simulation uncertainties.

2 LET relative permeability correlation

In 2005, a new versatile relative permeability correlation, i.e., LET, was introduced by Lomeland et al. [3] This correlation utilizes up to three parameters for each curve, i.e. L, E and T, giving the flexibility to match with relative permeability results from laboratory experiments or to generate upscaled relative permeability curves for field-scale simulation.

The LET relative permeability uses the normalized water saturation shown in Equation 1.

$$S_{wn} = \frac{S_w - S_{wi}}{1 - S_{wi} - S_{orw}} \tag{1}$$

In oil-water case, the L_o, E_o, T_o denotes the parameters for oil phase, while L_w, E_w, T_w denotes the parameters for water phase.

$$k_{row} = k_{ro}^{x} \frac{(1 - S_{wn})^{Lo}}{(1 - S_{wn})^{Lo} + E_o\,(S_{wn})^{To}} \tag{2}$$

$$k_{rw} = k_{ro}^{x} \frac{(S_{wn})^{Lw}}{(S_{wn})^{Lw} + E_w\,(1 - S_{wn})^{Tw}} \tag{3}$$

Employing the LET correlation, the relative permeability curve can be seen as in **Fig. 2**, where L describes the shape of lower part, E describes the middle part, and T describes the upper part of the relative permeability curve [1].

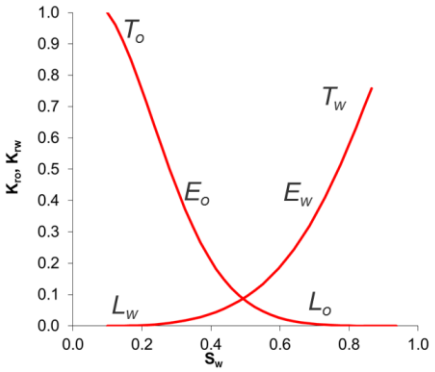

Fig. 2. LET parameters in relative permeability. [1]

Experience using the LET correlation indicates that the parameter L>=1, E>0, and T>=0.5 [3].

2.1. Generating different LET combinations

To create different combinations of the LET parameters resulting in similar relative permeability curves, 300 samples of water relative permeability curves were evaluated with properties presented in **Table 1.** and plotted in **Fig. 3**.

Table 1. Water relative permeability parameters.

Parameters	Value range
krw@Sorw	0.01 – 1
Swi	0.01 – 0.4
Sorw	0.01 – 0.4
Lw	1 – 12
Ew	1 – 12
Tw	1 – 12

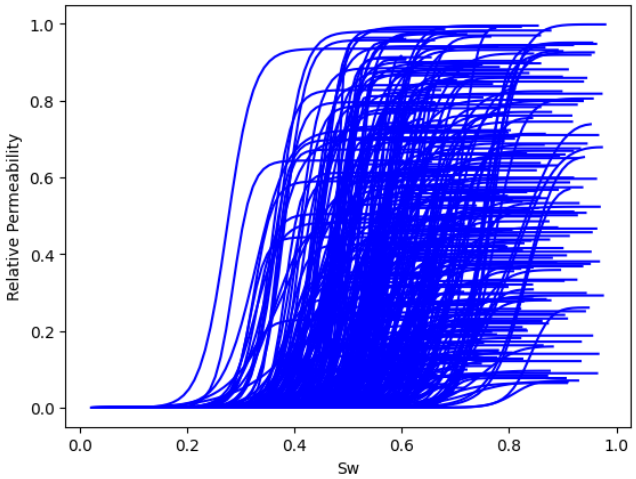

Fig. 3. Sampled water relative permeability curves.

Each of the samples was given a fixed range of L_w from 1 to 12 with a step of 0.01 (1100 realizations). With the known S_{wi}, S_{orw}, $k_{rw}@S_{orw}$, and L_w, the E_w and T_w can be determined by curve fit to the initial relative permeability curve. The initial parameters for one sample out of the sampled water relative permeability combinations are shown in **Table 2**.

Table 2. Initial water relative permeability parameters for Sample 241.

Parameters	K_{rw} @S_{orw}	S_{wi}	S_{orw}	L_w	E_w	T_w
Sample-241	0.267	0.182	0.219	7.42	11.25	6.25

From the results of 1100 different LET combinations, in the normal scale, the water relative permeability does not show any differences. However, in the semi-log scale, the water relative permeability at initial water saturation varies from 10^{-7} to 10^{-20} for different realizations, which is lower than the analytical relative permeability precision. Based on the **Fig. 4**, the results presented a possibility of a similar relative permeability curve with different LET combinations.

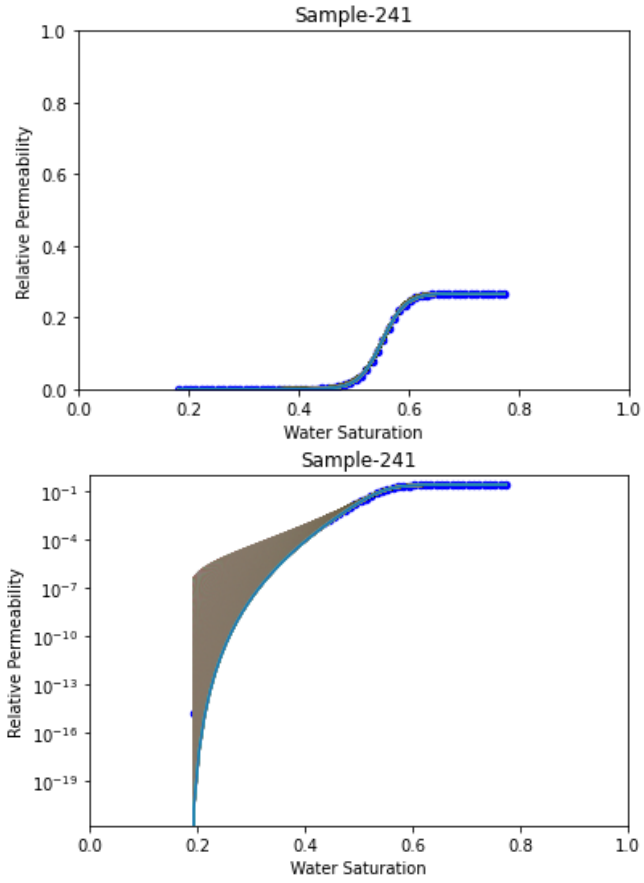

Fig. 4. Sample-241 water relative permeability curve with 1100 different combination

2.2 Relationship between L, E, and T

To further understand the relationship between LET parameters, all different combinations were considered to see the relationship. The established relationship between L_w versus E_w and L_w versus T_w, for one of the samples, is shown in **Fig. 5** and **Fig. 6** respectively.

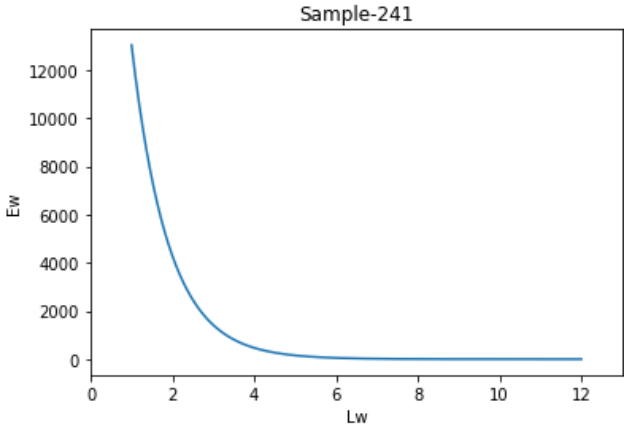

Fig. 5. Sample-241 water relative permeability L_w vs E_w

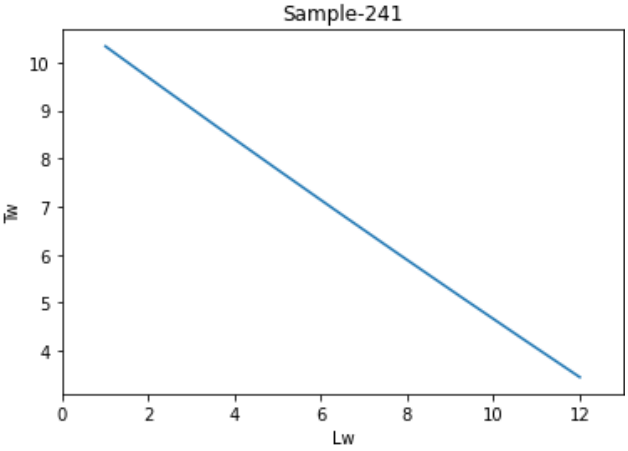

Fig. 6. Sample-241 water relative permeability L_w vs T_w

The L_w versus E_w can also be plotted into a semi-log plot as in **Fig. 7**. These results show that to generate different combinations, there is a negative linear relationship between L_w versus log (E_w) and L_w versus T_w.

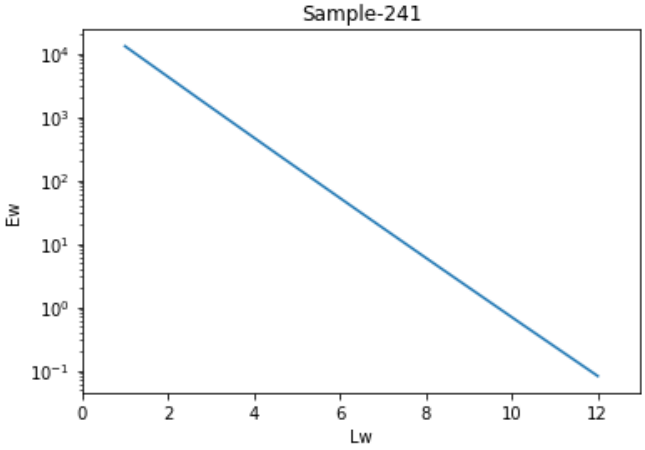

Fig. 7. Sample-241 water relative permeability L_w vs E_w

This means that a lower value of L will give a higher value of E and T, and vice versa. These relations are also applicable to the other phase of the relative permeability curve.

2.3 E and T multivariate regression and applications

By using the results from the relationship between L_w vs E_w and L_w vs T_w, a multivariate regression analysis was performed to define E and T parameters. In this analysis the initial L, E, T, $k_{rw}@S_{orw}$, S_{wi}, S_{orw}, and the desired L were used as input variables.

The multivariate regression results versus curve fitting results for *log (*E*)* and T parameters are presented in **Fig. 8** and **Fig. 9**, respectively. These results show an R^2 of 0.997 for both *log(*E*)* and T parameters.

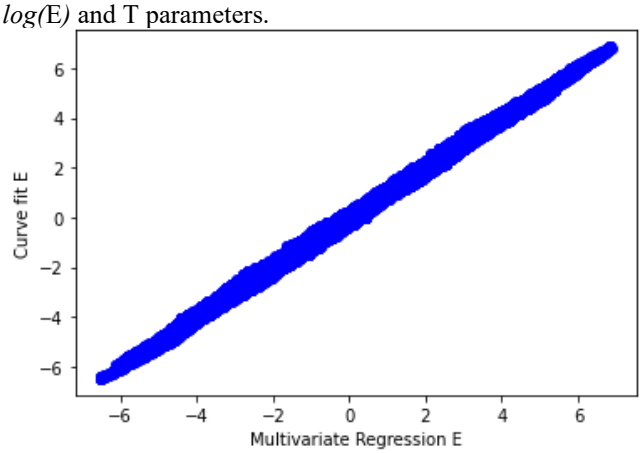

Fig. 8. Multivariate regression results compared with curve fitting results for E parameter.

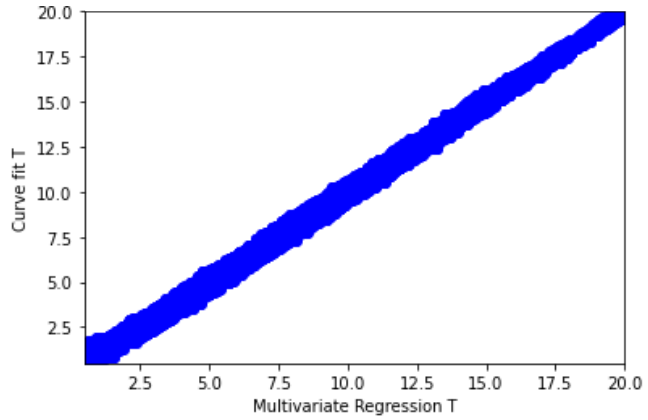

Fig. 9. Multivariate regression results compared with curve fitting results for T parameter.

The overall results exhibit dependency between the parameters, i.e. the parameter of L, E and T can be updated simultaneously by simply changing the L-parameter. The objective of creating multivariate regression of this dependency is to substitute the need to curve fit for each time the parameter is changed.

The proposed parameter adjustment combined with field scale trend modelling introduced by Ebeltoft et al. [1] can be useful to update the relative permeability and improve the uncertainty of the relative permeability parameters at field level.

The water relative permeability parameters in combination with the field trend models for sample 241 are presented in **Fig. 10**. One can see that the initial L_w is outside the field trend of L_w vs initial water saturation, therefore it requires some adjustment to the possible combination. By adjusting the L_w and using the relationship between L_w vs E_w and L_w vs T_w, the E_w and T_w is also adjusted simultaneously.

After applying the trend model, only 24 combinations out of 1100 different combinations are possible to follow the field trend. The combination with the field trend model [1] will provide a more robust approach to define the LET parameters for field scale simulations.

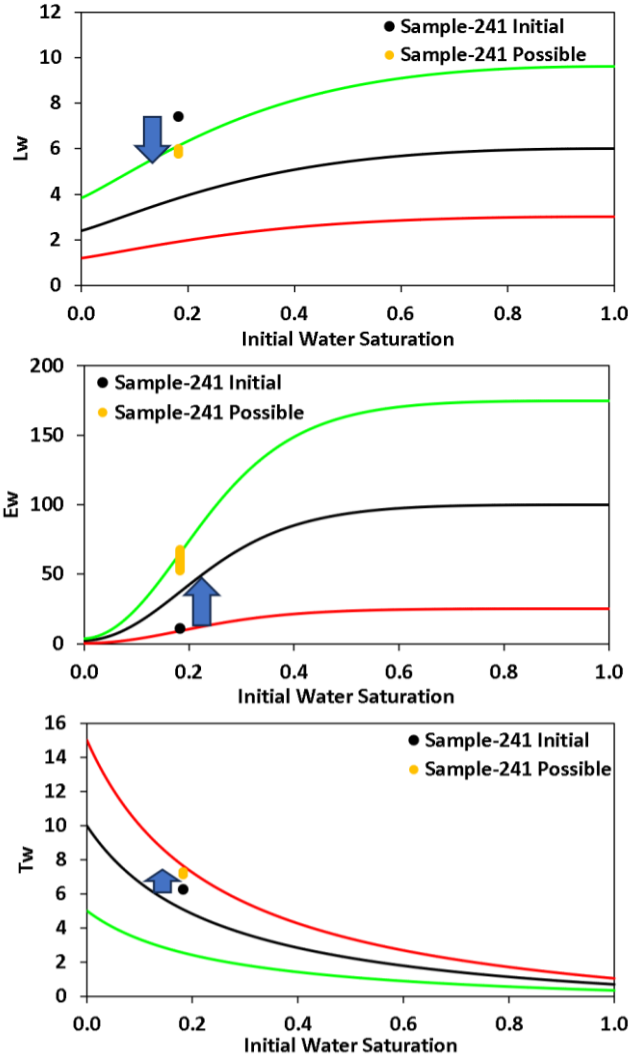

Fig. 10. Adjustment of sample-241 to the possible combination based on field trend model for L_w vs. initial water saturation (top), E_w vs. initial water saturation (middle), T_w vs. initial water saturation (bottom).

3 Case studies

For further investigations, different combinations of relative permeability were tested out in two field-scale reservoir models, i.e. the UNISIM-I-D field with oil and water system, and the Norne field with oil, gas and water system. The L-parameter of each phase is adjusted to ±0.5 from the original value. The E and T parameters follow the adjustment based on the LET relationship described in subsection 2.2.

For the case studies, Sendra cloud coreflooding simulator and Open Porous Media (OPM) 2022.10 reservoir simulator were used to perform the coreflood and field-scale numerical simulations. ResInsight was used for reservoir visualization.

3.1. UNISIM-I field model

UNISIM-I field model is a two-phase oil-water system field based on the geomodel of Namorado Field, located in Campos Basin in Brazil (**Fig. 11**) [7].

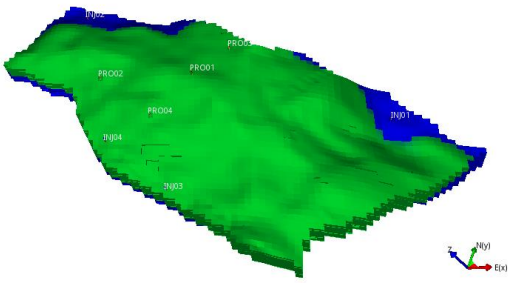

Fig. 11. The UNISIM-I field reservoir model.

The initial relative permeability parameters of UNISIM-I are presented in **Table 3** and **Fig. 12.**

Table 3. UNISIM-I field oil-water relative permeability variables.

Parameters	**K_{rw} @S_{orw}**	**S_{wi}**	**S_{orw}**	**L_w**	**E_w**	**T_w**
Water relative permeability	0.42	0.17	0.18	3.05	2.58	0.93
Parameters	**K_{ro} @S_{wi}**	**S_{wi}**	**S_{orw}**	**L_o**	**E_o**	**T_o**
Oil relative permeability	0.58	0.17	0.18	2.11	2.42	0.97

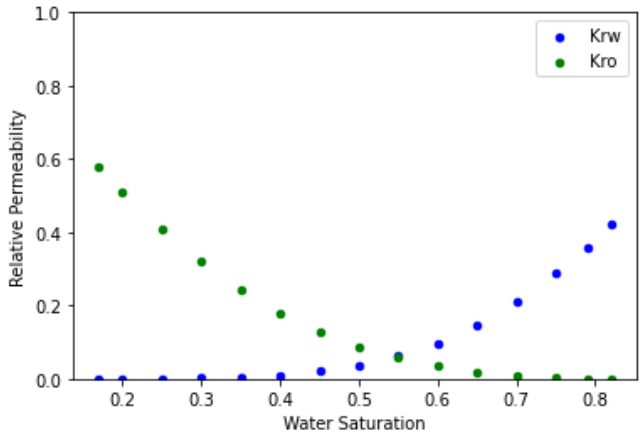

Fig. 12. UNISIM-I oil-water relative permeability.

The generated relative permeability parameter combinations with ±0.5 from base (Case-2) L_w and L_o are shown in **Table 4**, where Case-0 represents the -0.5 L_w and +0.5 L_o and Case-4 represents the +0.5 L_w and -0.5 L_o.

Moreover, the resulting relative permeability and coreflooding results for all cases are presented in **Fig. 13** and **Fig. 14**.

Table 4. The relative permeability combinations for UNISIM-I.

Relative Permeability	**L_w**	**E_w**	**T_w**	**L_o**	**E_o**	**T_o**
Case-0	2.55	3.65	1.06	2.61	1.63	0.81
Case-1	2.80	3.07	0.99	2.36	1.98	0.89
Case-2 (UNISIM-I)	3.05	2.58	0.93	2.11	2.42	0.97
Case-3	3.30	2.19	0.87	1.86	2.99	1.06
Case-4	3.55	1.86	0.81	1.61	3.72	1.15

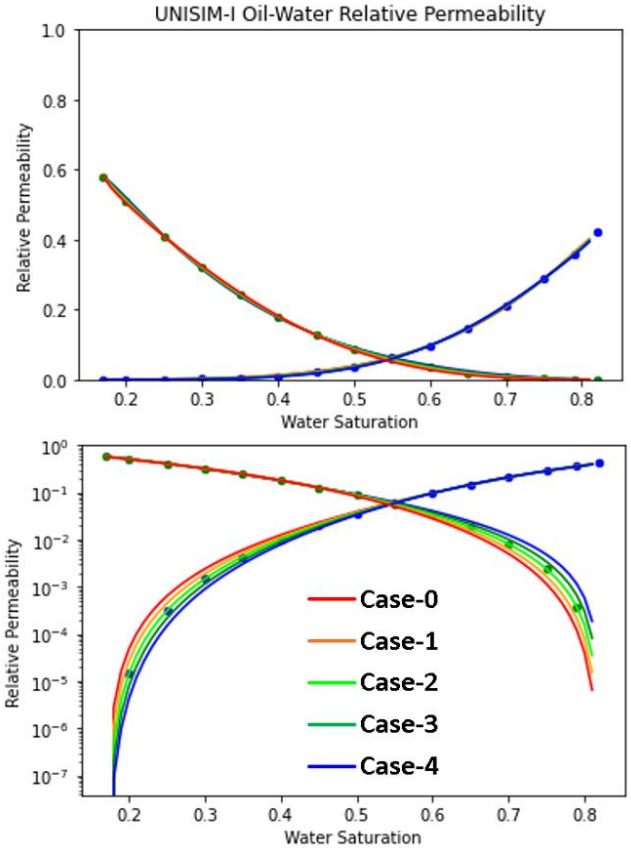

Fig. 13. UNISIM-I relative permeability combinations shown in normal (top) and semi-log (bottom) scales.

3.1.1 Coreflood simulation results

The steady-state water displacing oil coreflood simulation is carried out with the properties of the UNISIM-I field model and relative permeability curves. **Table 5** shows the UNISIM-I properties that were used for the coreflooding simulation.

Table 5. UNISIM-I properties for coreflooding simulation.

Properties	Values
Diameter	3.75 cm
Length	25 cm
Average porosity	13.6 %
Average permeability	132.5 mD
Water density	1.021 g/cc
Water viscosity	0.36 cP
Oil density	0.78 g/cc
Oil viscosity	1.2 cP

The results of the coreflooding are shown in **Fig. 14**

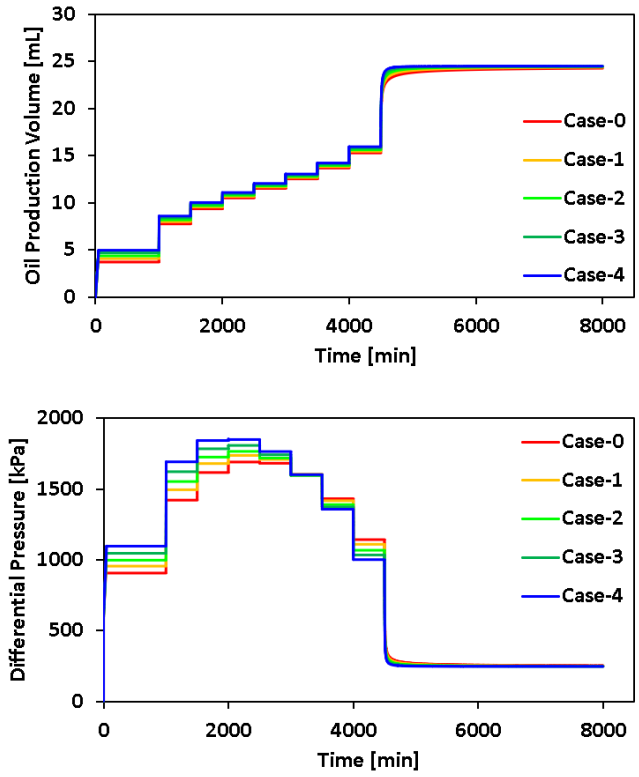

Fig. 14. UNISIM-I oil-water imbibition coreflooding production volume (top) and differential pressure (bottom) results.

As shown in **Fig. 14**, the effect of different LET parameters combinations for imbibition coreflooding can be seen from the beginning to the end of the simulation. Among the different scenarios, Case-4 (blue curve) and Case-0 (red curve) yield the highest and lowest oil production volume, respectively. Furthermore, the total oil production and recovery factors for various relative permeability cases are presented in **Table 6**. The obtained results show a difference of 0.68% in recovery factor between Case-4 (highest production) and Case-0 (lowest production).

Table 6. UNISIM-I coreflooding recovery results for various cases.

Relative Permeability	Total Oil Production [cc]	Recovery Factor [%]
Case-0	24.26	77.60
Case-1	24.36	77.92
Case-2 (UNISIM-I)	24.43	78.13
Case-3	24.46	78.25
Case-4	24.47	78.28

3.1.2 Field-scale simulation

The UNISIM-I model was simulated with an optimized well-control strategy from the beginning of 2013 until the end of 2037. The initial oil in place of the UNISIM-I model is 886.93 MMSTB. **Table 7** and **Fig. 15** present the field-scale simulation results that were carried out by using the LET parameters from **Table 4.**

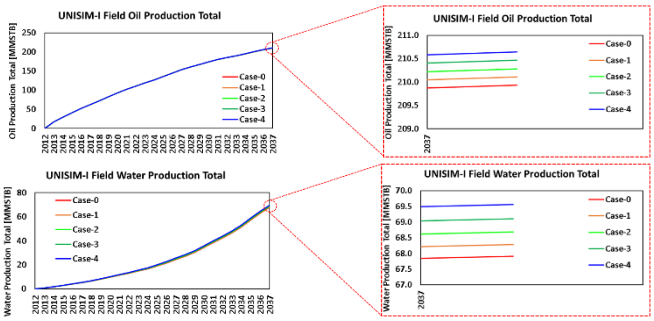

Fig. 15. UNISIM-I field simulation results.

The UNISIM-I field-scale simulation results exhibit similar results as the coreflooding simulation with Case-2 and Case-0 showing the highest and the lowest oil recovery, respectively.

Table 7. UNISIM-I field-scale recovery results.

Relative Permeability	Total Oil Production [MMSTB]	Recovery Factor [%]	Total Water Production [MMSTB]
Case-0	209.93	23.67	67.91
Case-1	210.11	23.69	68.29
Case-2 (UNISIM-I)	210.28	23.71	68.69
Case-3	210.47	23.73	69.11
Case-4	210.64	23.75	69.56

The field-scale simulation shows only a 0.71 MMSTB difference in oil production, i.e. 0.08% recovery difference, between the best and worst cases. Here, changes in relative permeability affects the water production in addition to the oil production with a difference of 1.65 MMSTB.

The results exhibit that the combination of low L_w and high L_o leads to lower oil recovery and lower water production, and vice versa. As presented in **Fig. 13** semi-log relative permeability, Case-0 with low L_w and high L_o initially have higher water relative permeability than Case-4 with similar oil relative permeability, therefore the total relative permeability of Case-0 is higher than Case-4 until midway. At the midway point, both cases have the same relative permeability. After the midway, Case-4 has higher oil relative permeability than Case-0 with similar water relative permeability, which resulted in Case-4 having a higher total relative permeability than Case-0.

By looking at the total relative permeability difference, it can be concluded that Case-0 will have the ability to flow fluid higher than Case-4 until midway and Case-4 will be leading at the end of field drainage.**3.2. Norne field model**

Norne field is located in blocks 6608/10 and 6508/10 on a horst block in the southern part of the Nordland II in the Norwegian Sea. The full field model was published in 2013 as a benchmark model with real data to allow researchers to engage with the most realistic problems and challenges [8]. Norne field is a three-phase fluid system, oil reservoir with gas cap and aquifer (**Fig. 16**).

The initial relative permeability parameters associated with the Norne field for oil-water and gas-oil cases are presented in **Table 8** and **Table 9**, respectively. The respective initial relative permeability curves are also shown in **Fig. 17** and **Fig. 18**.

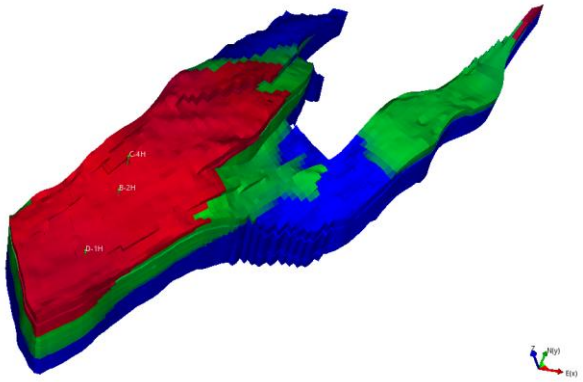

Fig. 16. The Norne field reservoir model.

Table 8. The initial oil-water relative permeability variables for Norne field.

Parameters	**K_{rw} @S_{orw}**	**S_{wi}**	**S_{orw}**	**L_w**	**E_w**	**T_w**
Water relative permeability	0.50	0.00	0.00	1.5	7.0	1.5
Parameters	**K_{ro} @S_{wi}**	**S_{wi}**	**S_{orw}**	**L_o**	**E_o**	**T_o**
Oil relative permeability	1.00	0.00	0.00	3.5	3.0	1.0

Table 9. The initial gas-oil relative permeability variables for Norne field.

Parameters	**K_{rg} @S_{org}**	**S_{org}**	**S_{gro}**	**L_g**	**E_g**	**T_g**
Gas relative permeability	0.95	0.00	0.00	2.0	1.5	0.9
Parameters	**K_{ro} @S_{gro}**	**S_{org}**	**S_{gro}**	**L_o**	**E_o**	**T_o**
Oil relative permeability	1.00	0.00	0.00	3.5	4.0	1.0

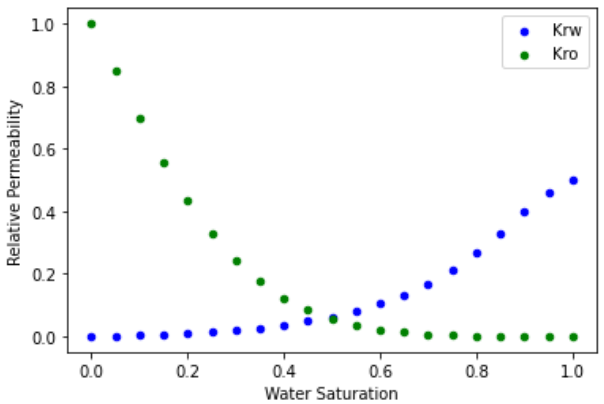

Fig. 17. The initial oil-water relative permeability curves for Norne field.

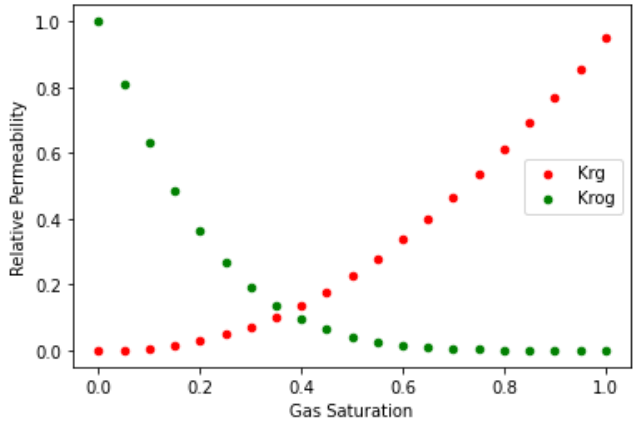

Fig. 18. The initial gas-oil relative permeability curves for Norne field.

The generated relative permeability parameter combinations with ±0.5 from the initial L_w, L_o and L_g, L_o are shown in **Table 10** and **Table 11**, respectively. Moreover, the corresponding relative permeability curves are plotted in **Fig. 19** and **Fig. 20**.

Table 10. The oil-water relative permeability parameter combinations for Norne field.

Relative Permeability	L_w	E_w	T_w	L_o	E_o	T_o
Case-0	1.00	10.95	1.70	4.00	2.18	0.88
Case-1	1.25	8.71	1.60	3.75	2.55	0.94
Case-2 (Norne)	1.50	7.00	1.50	3.50	3.00	1.00
Case-3	1.75	5.67	1.41	3.25	3.54	1.06
Case-4	2.00	4.62	1.33	3.00	4.18	1.12

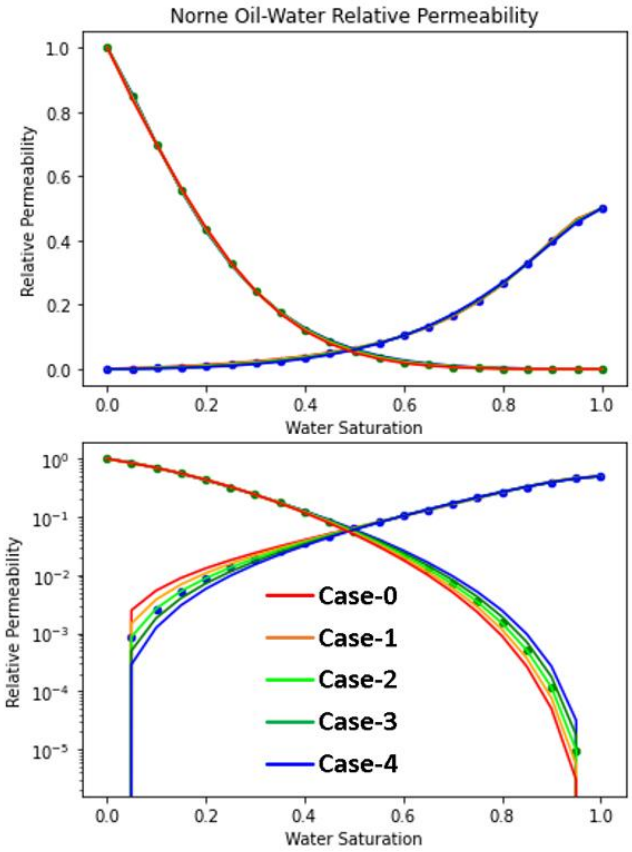

Fig. 19. Oil-water relative permeability combinations for Norne field.

Table 11. The gas-oil relative permeability parameter combinations for Norne field.

Relative Permeability	L_g	E_g	T_g	L_o	E_o	T_o
Case-0	1.50	2.47	1.13	4.00	2.97	0.90
Case-1	1.75	1.91	1.01	3.75	3.44	0.95
Case-2 (Norne)	2.00	1.50	0.90	3.50	4.00	1.00
Case-3	2.25	1.19	0.80	3.25	4.66	1.05
Case-4	2.50	0.94	0.70	3.00	5.44	1.11

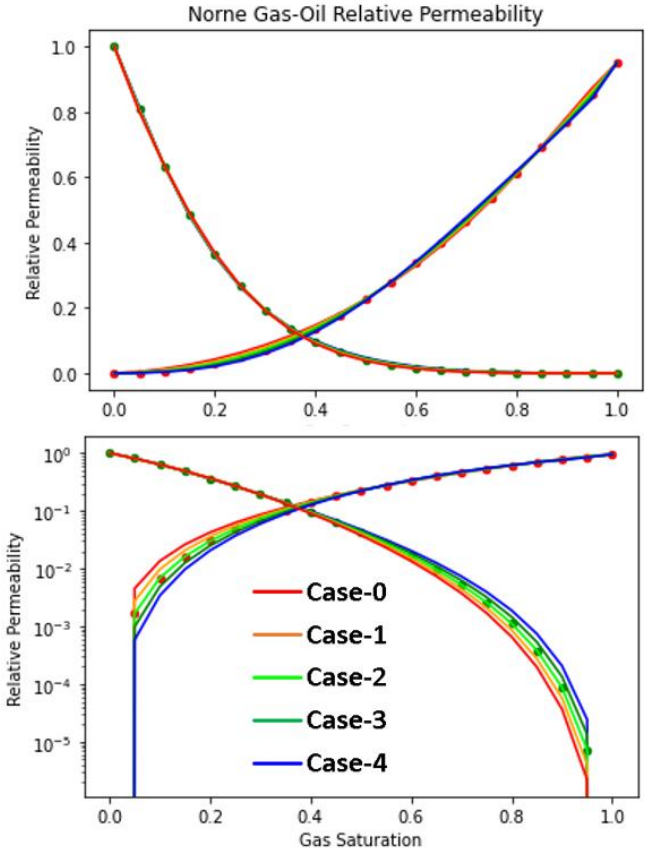

Fig. 20. Gas-oil relative permeability combinations for Norne field.

3.2.1 Coreflood simulation results

Since the Norne field is a three-phase fluid system reservoir, the coreflood simulation of water displacing oil, and gas displacing oil was carried out. **Table 12** and **Table 13** show the Norne properties that were used for the oil-water imbibition and gas-oil drainage coreflooding simulation.

Table 12. Norne properties for oil-water coreflooding simulations.

Properties	Values
Average porosity	24.3 %
Average permeability	390.28 mD
Water density	1.021 g/cc
Water viscosity	0.36 cP
Oil density	0.78 g/cc
Oil viscosity	1.2 cP

The coreflooding results of water displacing oil are shown in **Fig. 21**.

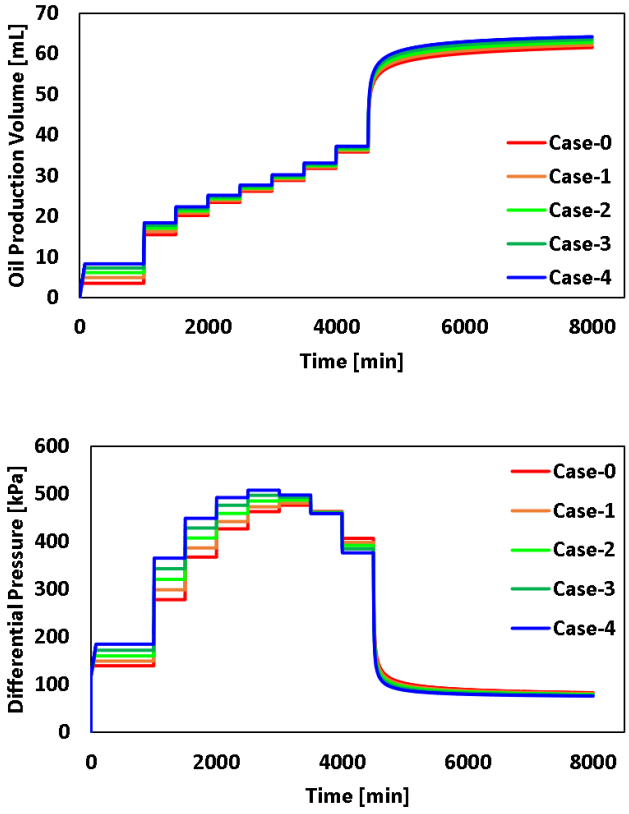

Fig. 21. Norne oil-water imbibition coreflooding results

Here, similar to the UNISIM-I results, Case-4 yields the highest oil production, while Case-0 results in the lowest oil production (**Table 14**). However, in case of Norne, the difference in recovery factor for oil-water imbibition coreflooding is higher, i.e. 3.94%, compared to the UNISIM model. This is due to the relative permeability saturation span being larger for Norne compared to the UNISIM model resulting in bigger differences between the LET combinations. Furthermore, the high recovery factor is due to the residual oil saturation, S_{orw}, which is 0 in the Norne model.

Table 13. Norne properties for gas-oil coreflooding simulations.

Properties	Values
Average porosity	24.3 %
Average permeability	390.28 mD
Gas density	0.0082 g/cc
Gas viscosity	0.0288 cP
Oil density	0.78 g/cc
Oil viscosity	1.2 cP

Table 14. Norne oil-water imbibition coreflooding recovery results.

Relative Permeability	Total Oil Production [cc]	Recovery Factor [%]
Case-0	61.51	91.68
Case-1	62.13	92.60
Case-2 (Norne)	62.80	93.60
Case-3	63.48	94.61
Case-4	64.15	95.62

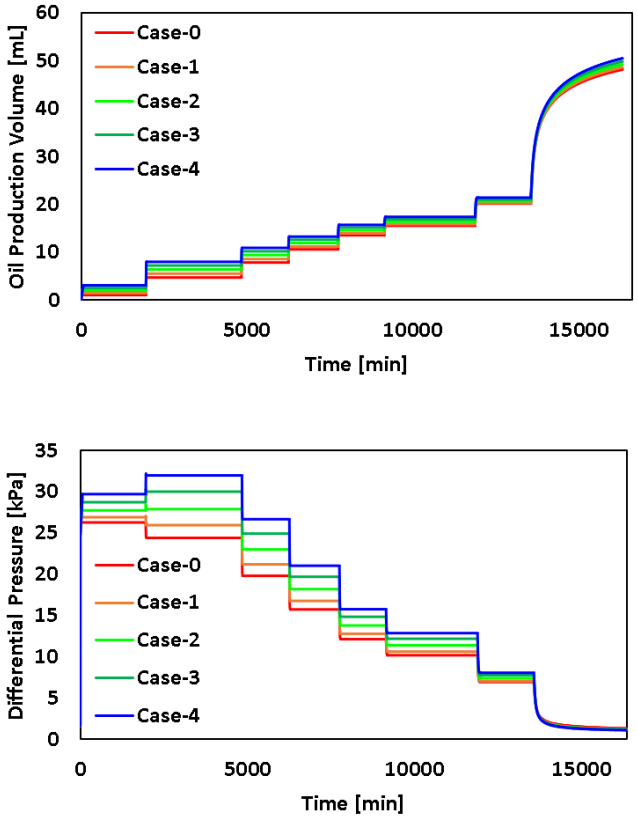

Fig. 22. Norne gas-oil drainage coreflooding results

With the combination from **Table 11**, the gas-oil drainage coreflooding simulation was performed. **Fig. 22** and **Table 15** present the coreflooding results, which shows the same behaviour as all previous coreflood simulations where Case-0 (Low L_g, High L_o) and Case-4 (High L_g, Low L_o) yield lowest and highest total oil production.

With these consistent results, one can conclude that, for coreflooding simulation, the production favours the oil phase when L_o is low and vice versa. This is due to oil relative permeability end point, which is almost always higher than the relative permeability for displacing phase. Another interesting observation is the differential pressure, where the volume will differ significantly between cases at the beginning of coreflood simulation and diminish at the end of the simulation. This is because the core is saturated by the displacing fluid and started to reach the endpoint.

Table 15. Norne gas-oil drainage coreflooding recovery results

Relative Permeability	Total Oil Production [cc]	Recovery Factor [%]
Case-0	48.16	71.78
Case-1	48.61	72.44
Case-2 (Norne)	49.20	73.33
Case-3	49.82	74.26
Case-4	50.49	75.25

3.2.2 Field-scale simulation

The Norne field model was simulated using the same strategy as the benchmark model. The simulation was run from 1997 to the end of 2006. Initial oil in place of the Norne field model is 1.011 BSTB. The field-scale simulation was carried out by using the different combinations of LET parameters as shown in **Table 10** for the oil-water case and **Table 11** for the gas-oil case.

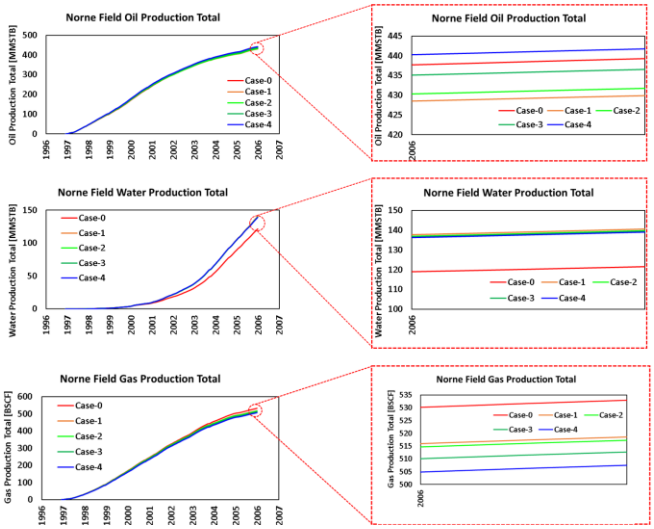

Fig. 23. Norne field simulation results

As shown in **Fig. 23**, the field-scale simulation results of the Norne field differ from coreflooding conclusion, where from Case-1 to Case-4 the oil production still follows the same

trend, while Case-0 shows higher oil production compared to Case-3.

The summary of gas-oil-ratio and total liquid production for field-scale simulation is shown in **Table 16**, from which one can see that, Case-0 and Case-4 present the highest and the lowest gas-oil-ratio, respectively. As anticipated, Case-0 exhibits the lowest liquid production, which is in line with UNISIM-I results.

Table 16. Norne gas-oil-ratio and liquid production results.

Relative Permeability	Gas Oil Ratio [BSCF/MMSTB]	Total Liquid Production [MMSTB]
Case-0	1.213	560.79
Case-1	1.206	570.48
Case-2 (Norne)	1.198	571.52
Case-3	1.174	575.93
Case-4	1.149	580.76

Based on Case-0 results, with higher gas production, it is inevitable that the production will favour oil production first before water production as shown in **Table 17**. This explains the higher gas flow with higher oil production.

Table 17. Norne field-scale recovery results.

Relative Permeability	Total Gas Production [BSCF]	Total Oil Production [MMSTB]	Total Water Production [MMSTB]
Case-0	532.94	439.27	121.52
Case-1	518.56	429.90	140.58
Case-2 (Norne)	517.27	431.75	139.78
Case-3	512.69	436.54	139.39
Case-4	507.49	441.74	139.02

According to the field simulation results from UNISIM-I (**Fig. 15**) and Norne field (**Fig. 23**), both fields show that at the initial stage of life of the field, the different combinations of L, E, and T parameters will not have a big effect, since it is still dominated by oil relative permeability which usually higher than the displacing fluid, i.e. water or gas. Entering the mid-life of the field, the difference starts to affect due to the difference in total relative permeability. The difference accumulates towards the late stage of field life.

4 Conclusion

LET relative permeability correlation is a powerful method to match the laboratory relative permeability results since it has the flexibility from 3 parameters, i.e. L, E and T. This study shows the potential of having different combination of L, E and T to generate a set of similar relative permeability curves that fits with laboratory relative permeability data points.

Here, a set of different LET combinations was evaluated and a new relation between L, E and T was obtained. Our evaluations show that to generate different combinations, the L parameter should be linearly inverse to the *log(*E*)* and T parameters. With the field trend model [1], the L, E and T parameter definition will be robust, able to adjust without significantly changing the relative permeability curves and obtain the potential L, E and T parameter combinations that are in the range of the field trend.

In the provided case studies, the effect of different L, E and T parameters in the UNISIM-I two-phase oil-water system model on core-scale and field-scale simulation results are in agreement. Our results show that lower L_o yields higher oil production in the UNISIM-I case, which is consistent on both core-scale and field-scale simulations. However, the effect in the Norne field is more complicated since it is a three-phase gas-oil-water system. In this case a lower L_g tends to result in more gas production, while a lower L_w and a higher L_o result in reduced liquid production.

The case studies also show that the uncertainty of different L, E and T combinations can be captured initially from the coreflooding simulations, and this is directly reflected in the field-scale simulations, i.e. the higher the differences on the core-scale, the higher the differences on the field-scale simulations. Moreover, the field simulation results show that the effect of different L, E and T combinations can be seen at the late stage of the field production. At the initial stage of the field, based on the usual shape of relative permeability curve, the oil relative permeability is dominant and therefore the different combinations of L, E and T will yield the same result. At the middle stage of the field, the different combination will take effect because the total relative permeability starts to differ, where the difference is accumulated until the late stage of the field.

5 Further Work

The combination set of L, E and T parameters together with the trend model can be incorporated with field analogues to reduce the uncertainty associated with relative permeability curves.

The author would like to acknowledge all Prores AS colleagues that have been very supportive, and Open Porous Media (OPM) and ResInsight as an integral part of the reservoir simulation and visualization in this study.

References

1. E. Ebeltoft, F. Lomeland, A. Brautaset, Å. Haugen, *Parameter Based SCAL – Analysing Relative Permeability for Full Field Application.* In *International Symposium of the Society of Core Analysts*, Avignon, France (2014)

2. A. T. Corey, *The Interrelation Between Gas and Oil Relative Permeabilities*, Prod. Monthly, **19 (1),** 38-41 (1954)

3. F. Lomeland, E. Ebeltoft, W. H. Thomas, *A New Versatile Relative Permeability Correlation*. In *International Symposium of the Society of Core Analysts*, Toronto, Canada (2005)

4. P. M. Sigmund, F. G. McCaffery, *An Improved Unsteady-State Procedure for Determining the Relative-Permeability Characteristics of Heterogeneous Porous Media*. Society of Petroleum Engineers Journal **19(01)**, 15-28 (1979)

5. G.L. Chierici, *Novel Relations for Drainage and Imbibition Relative Permeabilities. Society of Petroleum Engineers Journal*, **24(03)**, 275-276 (1984)

6. N. Burdine, *Relative Permeability Calculations from Pore Size Distribution Data*. Journal of Petroleum Technology **5**, 03, 71-78 (1953)

7. G. D. Avansi, D. J. Schiozer, *UNISIM-I: Synthetic Model for Reservoir Development and Management Applications*. International Journal of Modeling and Simulation for the Petroleum Industry, **9 (1)**, 21 – 30 (2015)

8. R. Rwechungura, E. Suwartadi, M. Dadashpour, J. Kleppe, B. Foss, *The Norne Field Case – A Unique Comparative Case Study*. In *SPE IntelligentEnergy Conference and Exhibition*, Utrecht, The Netherlands (2010)